

8. CHITOSAN-ALGINATE

BEADS

8.1. Chitosan-Alginate Amylase Beads

8.1.1. MATERIALS

Potassium dihydrogen phosphate, sodium hydroxide (NaOH), hydrochloric acid (HCl) (Qualigens Fine Chemicals, Mumbai, India) and soluble starch (Himedia Laboratories Pvt. Ltd., Mumbai, India) were used as received. Fungal α -amylase, sodium alginate, iodine, and potassium iodide were purchased from S. D. Fine-Chem Ltd., Mumbai, India. Chitosan (Chito Clear[®]) was the kind gift from Primex ehf, Ireland. All the other chemicals and solvents were of analytical grade and were used without further purification. Deionized double-distilled water was used throughout the study.

8.1.2. PREPARATION OF CHITOSAN-ALGINATE PEC BEADS

Chitosan-alginate PEC beads were produced from a pair of oppositely charged polysaccharides. A 1–3% w/v aqueous sodium alginate solution was prepared in deionized double-distilled water. An aqueous chitosan solution was prepared by dissolving the appropriate quantity of chitosan powder in 30 ml of 0.1 M HCl. Required quantity of enzyme (200 mg α -amylase in 50 ml of final chitosan solution) was dissolved

in small quantity of water and mixed with concentrated chitosan solution. Final concentration of chitosan solution was adjusted in the range of 1.5–2.5% w/v and was used after being degassed under a vacuum. Approximately 10 ml of enzyme containing chitosan was introduced into a 10-ml of glass syringe with a 18G×½” flat-cut hypodermic needle. The droplets were sheared off for 120 s at a flow rate 5 ml/min into 50 ml of sodium alginate solution. The resulting beads were allowed to harden for 30–60 min under gentle stirring (100 rpm) with small magnetic bar, decanted on Büchner funnel, rinsed with the deionized double-distilled water, and dried to a constant weight in vacuum desiccator (Tarsons Products Pvt. Ltd., Kolkata, India) at room temperature for 48 hours. The entire capsule formation procedure described herein was performed at ambient temperature. Different levels of independent variables (chitosan-, sodium alginate concentration, and hardening time) and the dependent variables (% entrapment, T_{50} , T_{90} , and particle size) with constraint used in the study are listed in Table 8.1. Figure 8.1 depicts the schematic representation of the PEC membrane formation which may be divided into three main classes: (i) primary complex formation; (ii) formation process within intracomplexes; (iii) intercomplex aggregation process. Prior mixing results in randomly arranged primary complex (due to secondary binding sources such as Coulomb forces (very rapid)), which upon further exposure converted to ordered secondary complex (due to formation of new bonds and/or the correction of the distortions of the polymer chain) and contains water molecules. Upon drying, PEC membrane undergoes intercomplex aggregation (because of hydrophobic interactions and/or drying), which constitute a network (Tsuchida, 1994).

Table 8.1: Process variables and responses with constraints for 3³ full factorial design.

Factors	Coded levels	Actual levels
A: Chitosan concentration (%w/v)	-1	1.5
	0	2.0
	1	2.5
B: Sodium alginate concentration (%w/v)	-1	1
	0	2
	1	3
C: Hardening time (min)	-1	30
	0	45
	1	60
Responses	Constraint	
M ₁ : % Entrapment	>90%	
M ₂ : T ₅₀ (min)	-	
M ₃ : T ₉₀ (min)	>48 min	
M ₄ : Particle size (mm)	-	

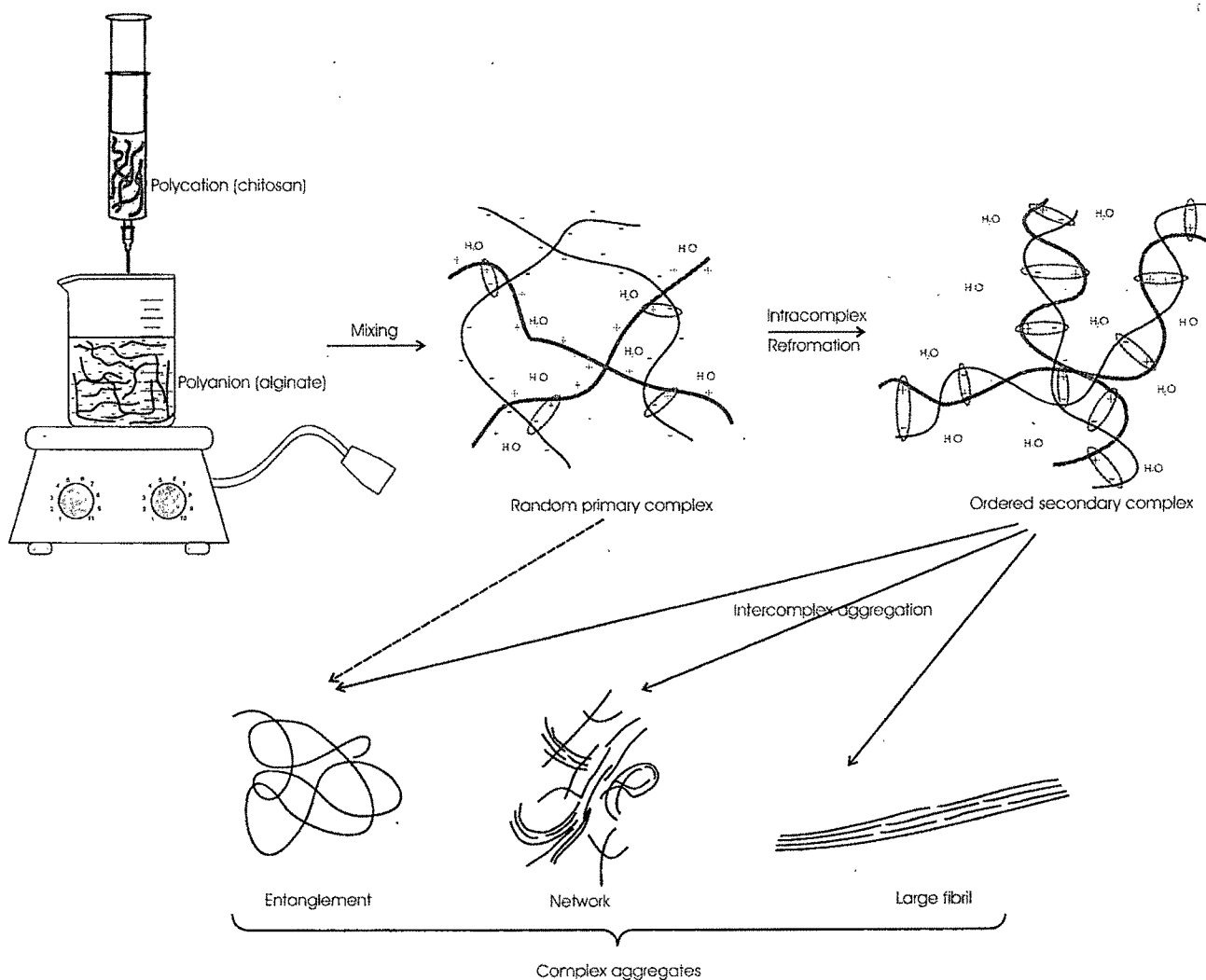


Figure 8.1: Schematic representation of PEC membrane formation.

8.1.3. 3³ FULL FACTORIAL DESIGN (FFD)

Statistical experimental designs have been in use for several decades (Plackett and Burman, 1946; Box and Hunter, 1957). These experimental layouts can be adopted at various phases of an optimization process, such as for screening experiments or for finding the optimal conditions for targeted results. The results analyzed by a statistically planned experiment are better acknowledged than those are carried out by the traditional single variable experiments. Response surface methodology has by now been established as a convenient method for developing optimum processes with precise conditions and has also minimized the cost of production of many a process with efficient screening of process parameters.

In order to attain the maximum entrapment and longer T₉₀, three-level full factorial designs was employed (number of runs $N=3^f$, where f is the number of independent variables). Before the application of the design, a number of preliminary trials were conducted to determine the conditions at which the process resulted in beads. To determine the experimental error, the experiment at the centre point was repeated three times at different days. The mean % entrapment, T₅₀, T₉₀, and particle size at the center-replicated points were 86.31±0.24%, 37.06±0.37 min, 43.09±0.39 min, and 1.43±1.07 mm respectively and showed good reproducibility of the process. For predicting the optimal region, a second order polynomial function was fitted to correlate relationship between variables and responses. The behavior of the system was explained by the following quadratic equation:

Eq. 8.1
$$Y = \beta_0 + \sum \beta_i x_i + \sum \beta_{ij} x_i x_j + \sum \beta_{ii} x_i^2$$

where Y is predicted response, β_0 is offset term (model constant), β_i is linear offset, β_{ii} is squared offset, β_{ij} is interaction effect, and x_i is dimensionless coded value of independent

Table 8.2: Matrix of 3³ full factorial design and results for the measured responses.

ES ^a	Factors/Levels			Responses			
	Chitosan (% w/v)	Sodium alginate (% w/v)	Hardening time (min)	% Immobilization	T ₅₀	T ₉₀	Particle Size (mm)
19	-1	-1	-1	82.21	29.20	33.50	1.020
11	-1	-1	0	81.48	33.30	38.40	1.013
24	-1	-1	1	81.18	36.40	43.70	1.011
31	-1	0	-1	85.22	34.70	40.50	0.960
23	-1	0	0	84.57	38.80	44.60	0.953
20	-1	0	1	84.26	42.40	49.20	0.950
7	-1	1	-1	88.55	40.50	46.50	0.910
16	-1	1	0	87.97	44.05	51.60	0.909
4	-1	1	1	87.61	48.10	55.60	0.909
29	0	-1	-1	83.66	27.20	33.50	1.530
5	0	-1	0	83.00	31.50	38.55	1.524
17	0	-1	1	82.71	34.40	40.40	1.522
25	0	0	-1	86.85	33.30	38.30	1.440
21	0	0	0	85.99	37.06	43.61	1.438
22	0	0	0	86.28	36.84	42.53	1.431
10	0	0	0	86.27	37.00	43.20	1.434
26	0	0	0	86.65	37.68	43.19	1.436
18	0	0	0	86.37	36.74	42.94	1.432
6	0	0	1	85.94	40.15	47.20	1.431
13	0	1	-1	90.38	38.70	44.20	1.380
27	0	1	0	89.88	43.20	49.50	1.375
1	0	1	1	89.51	46.55	52.95	1.370
15	1	-1	-1	85.35	26.30	31.30	1.940
3	1	-1	0	84.74	30.30	36.10	1.935
2	1	-1	1	84.46	33.05	38.50	1.933
9	1	0	-1	88.93	31.80	37.30	1.810
30	1	0	0	88.42	35.40	41.50	1.805
14	1	0	1	88.11	38.80	44.30	1.802
28	1	1	-1	92.64	37.20	42.85	1.728
8	1	1	0	92.24	40.40	46.80	1.723
12	1	1	1	91.91	44.15	49.90	1.719

variables (X_i). From the quadratic equation, response surfaces were generated and the overlapping region of the responses with constraint was considered as the optimum region where the beads with desired criteria can be produced. The analysis of variance (ANOVA) was performed in order to determine significance of the fitted equation. All analytical treatments were supported by NCSS software (Hintze, 2003). The quality of fit

of the polynomial model equation was expressed by the adjusted coefficient of determination R_{adj}^2 . All experimental designs were randomized to exclude any bias. The process variables with their coded experimental values and the results of the responses are reported in Table 4.2, while the design is also shown geometrically in Figure 8.2.

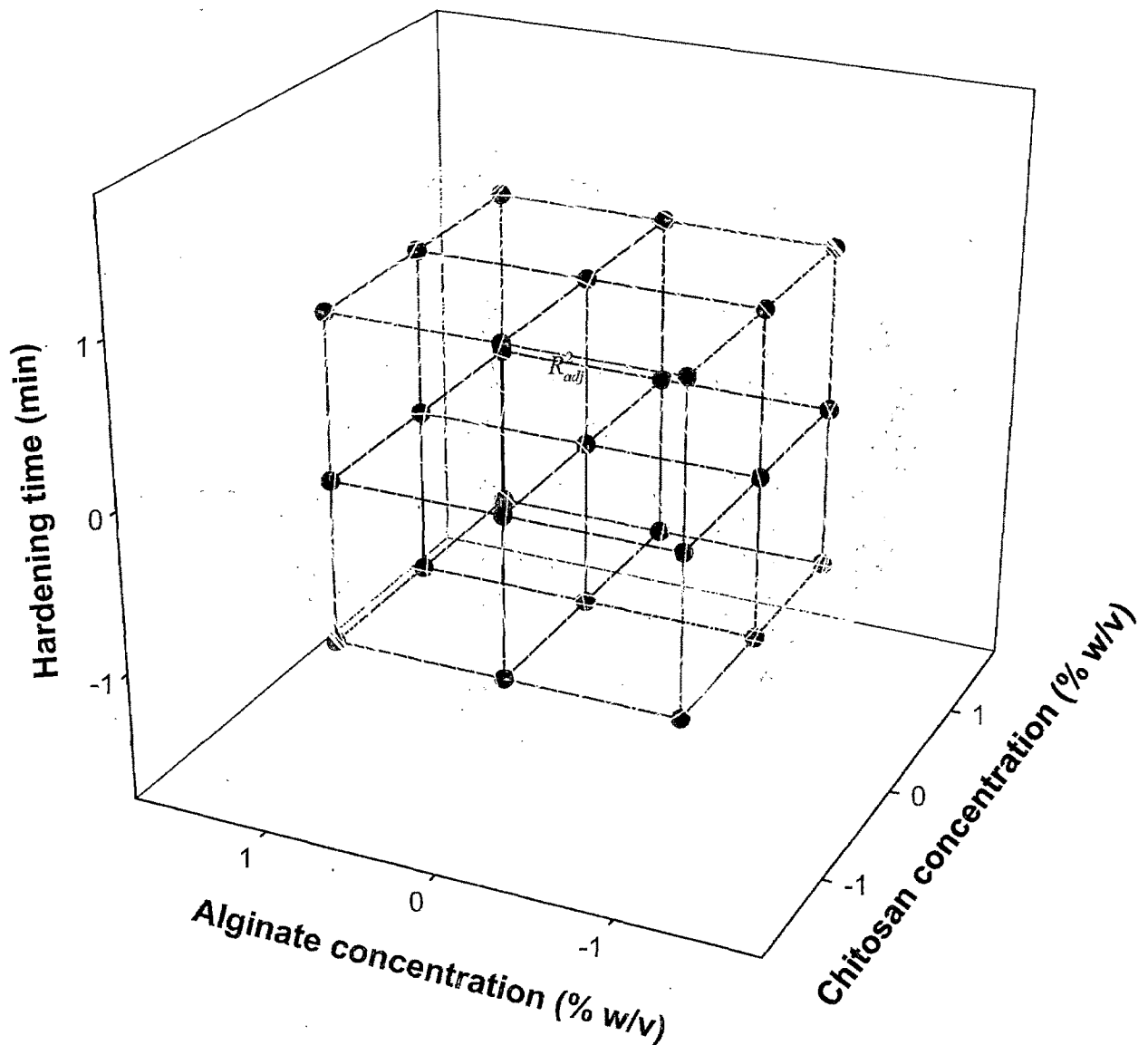


Figure 8.2: Three-dimensional view of 3^3 full factorial design.

8.1.4. CURVE FITTING

The 'in vitro' release pattern was evaluated to check the goodness of fit to the zero-order release kinetics (Eq. 8.2), first-order release kinetics (Gibaldi and Feldman, 1967; Wagner, 1969) (Eq. 8.3), Higuchi's square root of time equation (Higuchi, 1963) (Eq. 8.4), Korsmeyer-Peppas' power law equation (Korsmeyer et al., 1983; Peppas, 1985) (Eq. 8.5), and Hixson-Crowell's cube root of time equation (Hixson and Crowell, 1931) (Eq. 8.6). The goodness of fit was evaluated by r (correlation coefficient) values. For better understanding residual analysis (Pather et al., 1998) of above models was performed on the optimized formulation.

Eq. 8.2
$$Q_t = Q_0 + K_0 t$$

where Q_t is the amount of drug dissolved in time t , Q_0 is the initial amount of drug in the solution (most times, $Q_0=0$), K_0 is the zero order release constant and t is release time.

Eq. 8.3
$$Q_t = Q_0 e^{-K_1 t}$$

Where Q_t is the amount of drug dissolved in time t , Q_0 is the initial amount of drug in the solution, K_1 is the first order release constant and t is release time.

Eq. 8.4
$$Q_t = K_H \sqrt{t}$$

where Q_t is the amount of drug dissolved in time t , K_H is the Higuchi dissolution constant and t is release time.

Eq. 8.5
$$Q_t / Q_\infty = K_k t^n$$

where Q_t is the amount of drug dissolved in time t , Q_∞ is the amount of drug dissolved in ∞ time (the drug loaded in the formulation), Q_t / Q_∞ is the fractional release of the drug in time t , K_k is a constant incorporating structural and geometric characteristic of dosage form, n is the release (diffusional) exponent that depends on the release

mechanism and the shape of the matrix tested (Ritger and Peppas, 1987) and t is release time. Interpretation of diffusional exponent is given in Table 8.3.

Eq. 8.6
$$Q_0^{1/2} - Q_t^{1/2} = K_s t$$

where Q_0 is the initial amount of drug in the pharmaceutical dosage form, Q_t is the remaining amount of drug in pharmaceutical dosage form at time t , K_s is a constant incorporating the surface-volume relation and t is release time.

Table 8.3: Interpretation of Korsmeyer-Peppas power law release exponent.

Release exponent (n)	Drug transport mechanism	Rate as a function of time
0.5	Fickian diffusion	$t^{-0.5}$
$0.5 < n < 1.0$	Anomalous transport	t^{n-1}
1.0	Case-II transport	Zero order release
Higher than 1.0	Super Case-II transport	t^{n-1}

In order to understand the release mechanism, the release data of the optimized batch was fitted to empirical equations proposed by Kopcha (Kopcha et al., 1991) (Eq. 8.7),

Eq. 8.7
$$M = At^{1/2} + Bt$$

In the above equations, M ($\leq 70\%$) is the percentage of drug released at time t , while A and B are, respectively, diffusion and erosion terms. According to this equation, if diffusion and erosion ratio, $A/B=1$, then the release mechanism includes both diffusion and erosion equally. If $A/B>1$, then diffusion prevails, while for $A/B<1$, erosion predominates.

8.1.5. CHARACTERIZATION OF BEADS

8.1.5.1. Estimation of α -Amylase (Dextrinogenic Assay)

The iodine test of Smith and Roe (Smith and Roe, 1957; Hsiu et al., 1964) was modified as follows: Two ml of a 0.2% starch solution was added to 1.0 ml of enzyme diluted in 0.05 M phosphate buffer pH 6.8. The mixture was incubated for 3 minutes at 25° and then reaction was stopped with 1 ml of 1 N HCl. Finally, 20 ml of water and 0.5 ml of 0.01 N iodine solution prepared according to Rice (Rice, 1959) were added and the absorbance A was recorded on a spectrophotometer (Shimadzu UV-1601, Japan) at 660 nm. The instrument was adjusted to zero reading with iodine blank containing neither enzyme nor substrate. The dextrinogenic activity is expressed in arbitrary units as follows:

Eq. 8.8
$$D = [(A_B - A) / A_B] \cdot E$$

Where A_B is the absorbance of the starch-iodine complex in the absence of enzyme and E is the enzyme dilution. Best results were obtained when the enzyme solution was diluted in such a manner as to make the ratio $(A_B - A) / A_B$, approach 0.20-0.25.

8.1.5.2. Determination of Entrapment Efficiency

Entrapment efficiency was determined by dissolving the enzyme loaded beads in a magnetically stirred simulated gastric fluid (SGF) without enzyme (USP XXVI) for about 90 min. The resulting solution was centrifuged at 2500 rpm for 10 min (Remi Instruments Ltd, Mumbai, India), aliquots from the supernatant were adjusted to pH 6.8 using 0.01 M NaOH and diluted appropriately with 0.05 M phosphate buffer pH 6.8 and assayed (n=3) for enzyme content using dextrinogenic method. Entrapment efficiency was calculated as:

equivalent to about 40 mg of α -amylase were introduced to dissolution media and samples of 2 ml were collected at 0, 0.25, 0.50, 0.75, 1.0, 1.5, 2.0, 2.5, 3.0, 3.5, 4.0, 4.5, 5.0, 5.5 and 6.0 hr. Samples were filtered through whatman[®] filter paper #42 and assayed for enzyme content as before.

8.1.5.6. Fourier Transform Infra-Red Spectroscopy (FTIR)

IR transmission spectra were obtained using a FTIR spectrophotometer (FTIR-8300, Shimadzu, Japan). A total of 2% (w/w) of sample, with respect to the potassium bromide (KBr; S. D. Fine Chem Ltd., Mumbai, India) disc, was mixed with dry KBr. The mixture was ground into a fine powder using an agate mortar before compressing into KBr disc under a hydraulic press at 10,000 psi. Each KBr disc was scanned 16 times at 4 mm/s at a resolution of 2 cm^{-1} over a wavenumber region of 400–4000 cm^{-1} using Happ-Genzel apodization. The characteristic peaks were recorded.

8.1.5.7. Differential Scanning Calorimetry (DSC)

Differential scanning calorimetric analysis was used to characterize the thermal behavior of the isolated substances, empty and enzyme loaded beads. DSC thermograms were obtained using an automatic thermal analyzer system (DSC-60, Shimadzu, Japan). Temperature calibration was performed using indium as a standard. Samples were crimped in a standard aluminum pan and heated from 40–400 °C at a heating rate of 10 °C/min under constant purging of dry nitrogen at 30 ml/min. An empty pan, sealed in the same way as the sample, was used as a reference.

8.1.5.8. Scanning Electron Microscopy (SEM)

The purpose of SEM study was to obtain a topographical characterization of the beads. The beads were mounted on brass stubs using carbon paste. SEM photographs were taken with scanning electron microscope (JSM-5610LV, Jeol Ltd., Tokyo, Japan) at the required magnification at room temperature. The working distance of 39 mm was maintained and acceleration voltage used was 20 kV, with the secondary electron image (SEI) as a detector.

8.1.6. PREPARATION OF CAPSULE FORMULATION, PACKAGING, AND STABILITY STUDY

Accurately weighed chitosan-alginate beads equivalent to 40 mg of α -amylase were filled into a hard gelatin capsule manually. The joint of the capsule body and cap was carefully sealed by pressing them to fit in the lock mechanism. The capsules were packed in high density polyethylene (HDPE) bottles with polypropylene (PP) caps (foamed polyethylene and pressure sensitive liner). The capsules were subjected to stability testing according to the International Conference on Harmonization guidelines for zone III and IV. The packed containers of prepared capsules along with marketed formulation and bulk α -amylase were kept for accelerated ($40\pm 2^\circ\text{C}/75\pm 5\%$ relative humidity) and long term ($30\pm 2^\circ\text{C}/65\pm 5\%$ relative humidity) stability for up to 12 months. For accelerated and long term stability, desiccators containing saturated sodium chloride and potassium iodide solutions were kept into ovens at 40°C and 30°C to maintain a constant relative humidity of 74.68 ± 0.13 and 67.98 ± 0.23 , respectively. A visual inspection (for discoloration of capsule content), dissolution testing, and α -amylase content estimation was carried out every 15 days for the entire period of stability study.

8.2. Chitosan-Alginate Papain Beads

8.2.1. MATERIALS

Hammersten type casein (Himedia Laboratories Pvt. Ltd., Mumbai, India) and trichloroacetic acid (Qualigens Fine Chemicals, Mumbai, India) were used as received. Purified papain, sodium alginate, potassium chloride, dibasic sodium phosphate and citric acid were purchased from S. D. Fine-Chem Ltd., Mumbai, India. Chitosan (Chito Clear[®]) was the kind gift from Primex ehf, Ireland. All the other chemicals and solvents were of analytical grade and were used without further purification. Deionized double-distilled water was used throughout the study.

8.2.2. PREPARATION OF CHITOSAN-ALGINATE PEC BEADS

Chitosan-alginate PEC beads were produced from a pair of oppositely charged polysaccharides. A 1–3% w/v aqueous sodium alginate solution was prepared in deionized double-distilled water. An aqueous chitosan solution was prepared by dissolving the appropriate quantity of chitosan powder in 30 ml of 0.1 M HCl. Required quantity of enzyme (300 mg papain in 50 ml of final chitosan solution) was dissolved in small quantity of water and mixed with concentrated chitosan solution. Final concentration of chitosan solution was adjusted in the range of 1.13–2.87% w/v and was used after being degassed under a vacuum. Approximately 10 ml of enzyme containing chitosan was introduced into a 10-ml of glass syringe with a 18G×½” flat-cut hypodermic needle. The droplets were sheared off for 120 s at a flow rate 5 ml/min into 50 ml of

sodium alginate solution. The resulting beads were allowed to harden for 19.02–70.98 min under gentle stirring (100 rpm) with small magnetic bar, decanted on Büchner funnel, rinsed with the deionized double-distilled water, and dried to a constant weight in vacuum desiccator (Tarsons Products Pvt. Ltd., Kolkata, India) at room temperature for 48 hours. The entire capsule formation procedure described herein was performed at ambient temperature. Different levels of independent variables (chitosan-, sodium alginate concentration, and hardening time) and the dependent variables (% entrapment, T_{50} , T_{90} , and particle size) are listed in Table 8.4. Figure 8.3 depicts the schematic representation of the PEC membrane formation which may be divided into three main classes: (i) primary complex formation; (ii) formation process within intracomplexes; (iii) intercomplex aggregation process. Prior mixing results in randomly arranged primary complex (due to secondary binding sources such as Coulomb forces (very rapid)), which upon further exposure converted to ordered secondary complex (due to formation of new bonds and/or the correction of the distortions of the polymer chain) and contains water molecules. Upon drying, PEC membrane undergoes intercomplex aggregation (because of hydrophobic interactions and/or drying), which constitute a network (Tsuchida, 1994).

Table 8.4: Process variables 3-factor central composite design.

Factors	Coded levels	Actual levels
A: Chitosan concentration (%w/v)	-1.73	1.13
	-1	1.5
	0	2
	1	2.5
	1.73	2.87
B: Sodium alginate concentration (%w/v)	-1.73	0.27
	-1	1
	0	2
	1	3
	1.73	3.73
C: Hardening time (min)	-1.73	19.02
	-1	30
	0	45
	1	60
	1.73	70.98

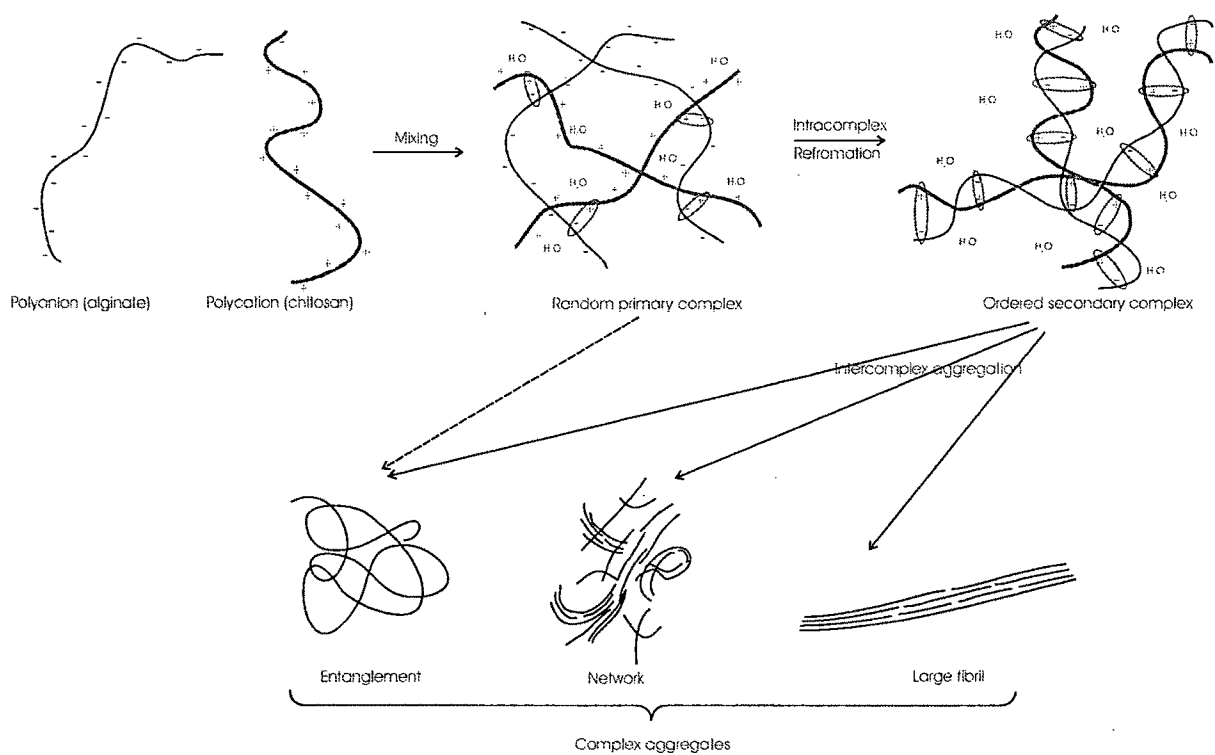


Figure 8.3: Schematic representation of PEC membrane formation.

8.2.3. CENTRAL COMPOSITE DESIGN (CCD)

Statistical experimental designs have been in use for several decades. These experimental layouts can be adopted at various phases of an optimization process, such as for screening experiments or for finding the optimal conditions for targeted results. The results analyzed by a statistically planned experiment are better acknowledged than those are carried out by the traditional single variable experiments. Response surface methodology has by now been established as a convenient method for developing optimum processes with precise conditions and has also minimized the cost of production of many a process with efficient screening of process parameters.

In order to attain the optimum response, three-level full factorial designs can be employed. However, these designs involve a very great number of runs ($N=3^f$, where f is the number of the independent variables) compared with the total quadratic coefficients to be determined, m . To alleviate this situation, central composite designs (CCD) can alternatively be used. The introduction of extra runs (star points and centre of design) to augment two-level factorial designs is to estimate the coefficients of the model equation in an efficient way. The number of runs to be made in both orthogonal or rotatable CCD are $N=2^f+2f+1$ (without replications), sensibly lower than three level factorial designs. For this reason, CCD are widely used in experimental optimization.

Before the application of the design, a number of preliminary trials were conducted to determine the conditions at which the process resulted in beads. To determine the experimental error, the experiment at the centre point was repeated three times at different days. The mean % entrapment, T_{50} , T_{90} , particle size, and composite index at the center-replicated points were $83.97\pm 1.00\%$, 37.09 ± 0.12 min, 43.22 ± 0.08 min, 1.38 ± 0.01 , and 23.43 ± 0.16 mm respectively and showed good reproducibility of the process. For predicting the optimal region, a second order polynomial function was fitted to correlate relationship between variables and responses. The behavior of the system was explained by the following quadratic equation:

Eq. 8.10

$$Y = \beta_0 + \sum \beta_i x_i + \sum \beta_{ij} x_i x_j + \sum \beta_{ii} x_i^2$$

where Y is predicted response, β_0 is offset term (model constant), β_i is linear offset, β_{ii} is squared offset, β_{ij} is interaction effect, and x_i is dimensionless coded value of independent variables (X_i). From the quadratic equation, response surfaces were generated and the overlapping region of the responses with constraint was considered as the optimum region where the beads with desired criteria can be produced. The analysis of variance (ANOVA) was performed in order to determine significance of the fitted equation. All

analytical treatments were supported by NCSS software. The quality of fit of the polynomial model equation was expressed by the adjusted coefficient of determination R_{adj}^2 . All experimental designs were randomized to exclude any bias. The process variables with their coded experimental values and the results of the responses are reported in Table 8.5, while the design is also shown geometrically in Figure 8.4.

Table 8.5: Matrix of central composite design and results for the measured responses.

Sr. No.	Factors/Levels			Responses			Transformed			Composite index
	Chitosan (% w/v)	Sodium alginate (% w/v)	Hardening time (min)	% Immobilization	T ₅₀	T ₉₀	Particle Size (mm)	% Immobilization	T ₉₀	
J-1	-1	-1	-1	80.48	29.31	33.94	1.09	6.87	3.79	10.66
J-2	-1	-1	1	78.77	36.59	43.30	1.21	0.00	23.60	23.60
J-3	-1	1	-1	87.23	40.47	46.49	0.92	33.82	30.35	64.17
J-4	-1	1	1	86.08	48.17	55.78	0.99	29.25	50.00	79.25
J-5	1	-1	-1	83.08	26.00	32.15	1.96	17.23	0.00	17.23
J-6	1	-1	1	83.09	32.67	38.79	1.91	17.27	14.05	31.31
J-7	1	1	-1	91.28	37.11	42.34	1.71	50.00	21.57	71.57
J-8	1	1	1	90.73	44.40	50.35	1.67	47.82	38.52	86.34
J-9	-1.73	0	0	81.01	40.21	46.18	0.71	8.99	29.69	38.68
J-10	1.73	0	0	88.71	34.03	39.43	2.04	39.76	15.41	55.17
J-11	0	-1.73	0	79.42	27.11	33.16	1.68	2.63	2.14	4.77
J-12	0	1.73	0	90.43	46.69	53.85	1.29	46.64	45.92	92.56
J-13	0	0	-1.73	85.66	29.88	34.48	1.42	27.55	4.93	32.48
J-14	0	0	1.73	84.50	42.81	49.08	1.48	22.92	35.83	58.75
J-15	0	0	0	83.61	36.97	43.22	1.36	19.35	23.43	42.79
J-16	0	0	0	83.21	37.09	43.30	1.39	17.76	23.59	41.34
J-17	0	0	0	85.11	37.21	43.14	1.36	25.35	23.27	10.66

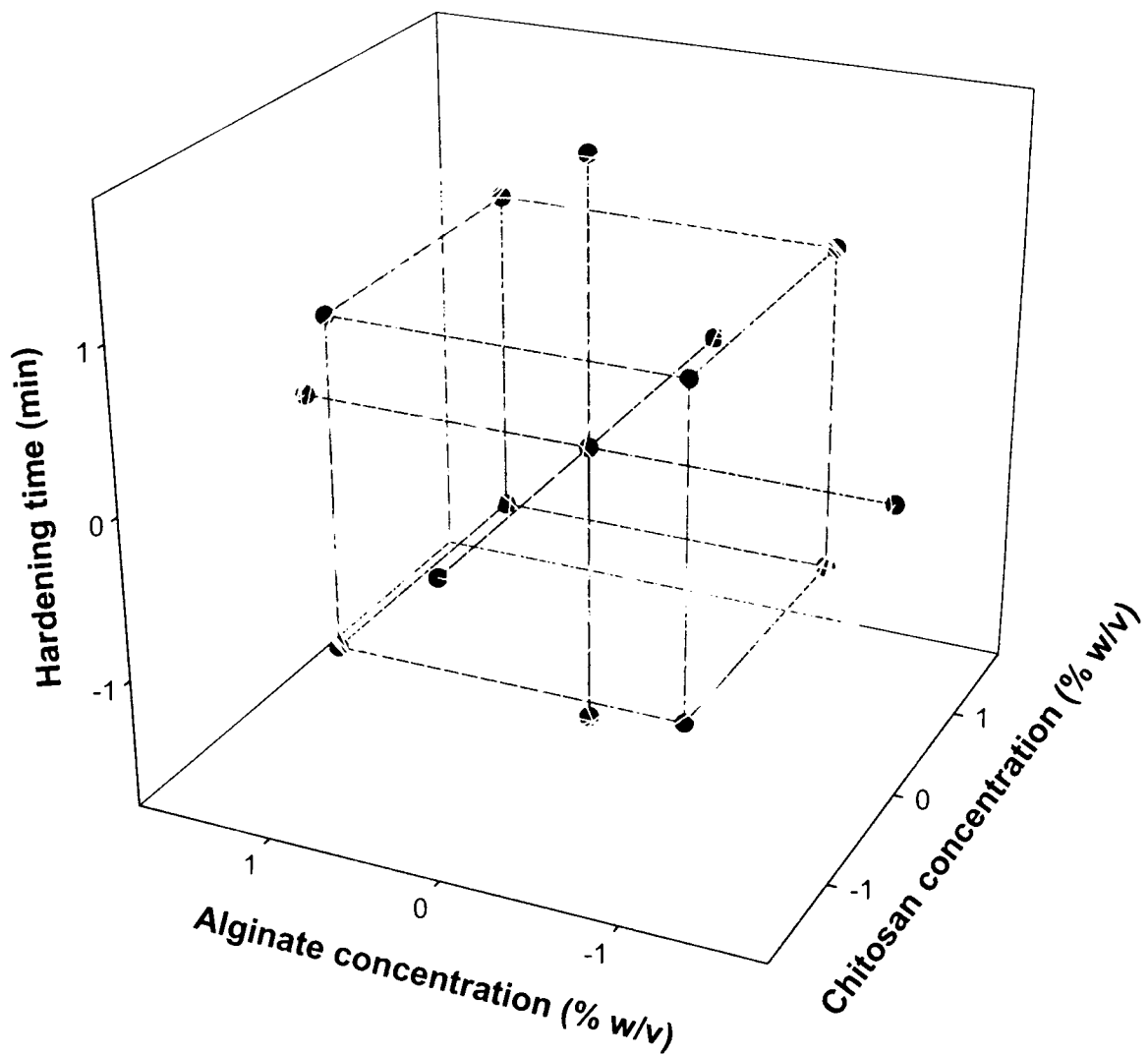


Figure 8.4: Three-dimensional view of 3-factor CCD.

8.2.4. COMPOSITE INDEX

On completion of the individual experiments, a weighted composite index was used to designate a single score utilizing two responses, i.e., % entrapment, and T_{90} . Derringer and Suich illustrated how several response variables can be transformed into one response (Derringer and Suich, 1980). The applications of one-sided transformations are also demonstrated by different researchers. The application of generalized distance function to incorporate several objectives into a single function has been reported (Shigeo et al.,

1994). As the relative contribution of each individual constraint to the “true” composite score was unknown, a decision was made to assign an arbitrary value of one-half to each of the two response variables (Taylor et al., 2000). The empirical composite index was devised to yield a score 100 for an optimum result for each of the two responses and each formulations result was transformed to a value between 0 and 50. For % entrapment, highest value (91.28) was assigned a score equal to 50, and lowest value (78.77) was assigned zero score. For T_{90} , lowest value (32.15) was assigned to zero score and the highest value (55.78) was assigned to 50. The batch having a highest composite index would be considered as the batch fulfilling the desired criteria. The raw data transformations were as follows:

Eq. 8.11 Transformed value of % entrapment or T_{90} = $\frac{Y_i - Y_{\min}}{Y_{\max} - Y_{\min}} \times 50$

where Y_i is the experimental value of individual response variable, Y_{\max} and Y_{\min} are maximum and minimum values of individual response variable, respectively.

Eq. 8.12 Composite index = $\left(\begin{array}{c} \text{transformed value} \\ \text{of \% entrapment} \end{array} \right) + \left(\begin{array}{c} \text{transformed} \\ \text{value of } T_{90} \end{array} \right)$

8.2.5. CURVE FITTING

The ‘*in vitro*’ release pattern was evaluated to check the goodness of fit to the zero-order release kinetics (Eq. 8.13), first-order release kinetics (Gibaldi and Feldman, 1967; Wagner, 1969) (Eq. 8.14), Higuchi’s square root of time equation (Higuchi, 1963) (Eq. 8.15), Korsmeyer-Peppas’ power law equation (Korsmeyer et al., 1983; Peppas, 1985) (Eq. 8.16), and Hixson-Crowell’s cube root of time equation (Hixson and Crowell, 1931) (Eq. 8.17). The goodness of fit was evaluated by r (correlation coefficient) values. For

better understanding residual analysis (Pather et al., 1998) of above models was performed on the optimized formulation.

Eq. 8.13
$$Q_t = Q_0 + K_0 t$$

where Q_t is the amount of drug dissolved in time t , Q_0 is the initial amount of drug in the solution (most times, $Q_0=0$), K_0 is the zero order release constant and t is release time.

Eq. 8.14
$$Q_t = Q_0 e^{-K_1 t}$$

Where Q_t is the amount of drug dissolved in time t , Q_0 is the initial amount of drug in the solution, K_1 is the first order release constant and t is release time.

Eq. 8.15
$$Q_t = K_{11} \sqrt{t}$$

where Q_t is the amount of drug dissolved in time t , K_{11} is the Higuchi dissolution constant and t is release time.

Eq. 8.16
$$Q_t / Q_\infty = K_k t^n$$

where Q_t is the amount of drug dissolved in time t , Q_∞ is the amount of drug dissolved in ∞ time (the drug loaded in the formulation), Q_t / Q_∞ is the fractional release of the drug in time t , K_k is a constant incorporating structural and geometric characteristic of dosage form, n is the release (diffusional) exponent that depends on the release mechanism and the shape of the matrix tested (Ritger and Peppas, 1987) and t is release time. Interpretation of diffusional exponent is given in Table 8.6.

Eq. 8.17
$$Q_0^{2/3} - Q_t^{2/3} = K_s t$$

where Q_0 is the initial amount of drug in the pharmaceutical dosage form, Q_t is the remaining amount of drug in pharmaceutical dosage form at time t , K_s is a constant incorporating the surface-volume relation and t is release time.

Table 8.6: Interpretation of Korsmeyer-Peppas power law release exponent.

Release exponent (n)	Drug transport mechanism	Rate as a function of time
0.5	Fickian diffusion	$t^{-0.5}$
$0.5 < n < 1.0$	Anomalous transport	t^{n-1}
1.0	Case-II transport	Zero order release
Higher than 1.0	Super Case-II transport	t^{n-1}

In order to understand the release mechanism, the release data of the optimized batch was fitted to empirical equations proposed by Kopcha (Kopcha et al., 1991) (Eq. 8.18),

Eq. 8.18
$$M = At^{1/2} + Bt$$

In the above equations, M ($\leq 70\%$) is the percentage of drug released at time t , while A and B are, respectively, diffusion and erosion terms. According to this equation, if diffusion and erosion ratio, $A/B=1$, then the release mechanism includes both diffusion and erosion equally. If $A/B>1$, then diffusion prevails, while for $A/B<1$, erosion predominates.

8.2.6. CHARACTERIZATION OF BEADS

8.2.6.1. Estimation of papain (Dextrinogenic assay)

Activity of papain was analyzed with casein according to the modified method of An et al (An et al., 1994). A reaction mixture containing 5 ml of 1% w/v casein (in 0.05M dibasic sodium phosphate; pH was adjusted to 6.0 ± 0.1 using 0.05M citric acid) was pre-incubated at 40°C for 10 min. Different aliquots of enzyme in buffer (pH 6.0 ± 0.1 , containing 3.55 g dibasic sodium phosphate, 7.0 g disodium ethylenediaminetetraacetate, and 3.05 g cysteine hydrochloride in 500 ml) and buffer solution was then added, and incubated at 40°C for 60 minutes. The total volume of the reaction mixture, including enzyme, was maintained at 7 ml. The reaction was terminated by adding 3 ml of cold

(4°C) 30% w/v trichloroacetic acid (TCA). After allowing unhydrolyzed proteins to precipitate at 4°C for 30 minutes, samples were centrifuged at 5000 rpm for 5 minutes (Remi Instruments Ltd, Mumbai, India). TCA-soluble proteins were recovered in the supernatant and absorbance due to tyrosine content was measured at 280 nm. Blank was prepared separately for each concentration where in the papain was inactivated by adding TCA before the addition of papain. Enzyme activity was expressed as difference of the absorbance between sample and blank at 280 nm (ΔA_{280}).

8.2.6.2. Determination of entrapment efficiency

Entrapment efficiency was determined by dissolving the enzyme loaded beads in a magnetically stirred simulated gastric fluid (SGF) without enzyme (USP XXVI) for about 90 min. The resulting solution was centrifuged at 2500 rpm for 10 min (Remi Instruments Ltd, Mumbai, India), aliquots from the supernatant were adjusted to pH 6.0±0.1 using 0.01 M NaOH and diluted appropriately with 0.05 M phosphate buffer pH 6.0±0.1 and assayed (n=3) for enzyme content using above method. Entrapment efficiency was calculated as:

$$\text{Eq. 8.19} \quad \text{Entrapment efficiency} = \frac{\text{Enzyme loaded}}{\text{Theoretical enzyme loading}} \times 100$$

8.2.6.3. Determination of T₅₀ and T₉₀

Time required for 50 (T₅₀) and 90 (T₉₀) percent of enzyme release were used to evaluate the onset and duration of action respectively. For optimization purpose, dissolution study of all batches was carried out in 500 ml of SGF without enzyme using the USP XXVI dissolution apparatus 2 (TDT-60T, Electrolab, Mumbai, India) at 37±0.5 °C with paddle

speed of 75 rpm. Accurately weighed samples (n=3) equivalent to about 40 mg of papain were subjected to dissolution, aliquots of 2 ml were collected, and assayed at 0, 5, 10, 15, 20, 25, 30, 35, 40, 45, 50, 55, 60 and 65 min. T₅₀ and T₉₀ were found by extrapolating the % enzyme released versus time plot.

8.2.6.4. Particle size measurements

The particle sizes of 50 gel beads were measured with a gauge type micrometer (0.01 mm least count, Durga Scientific Pvt. Ltd., Vadodara, India) for each formulation and the mean particle size was determined.

8.2.6.5. Effect of pH on release profile

To study the effect of pH on papain release profile from PEC, 'in vitro' dissolution study was carried out as before using 500 ml of different pH media (SGF without enzyme pH 1.2, phosphate buffer pH 4.0, simulated intestinal fluid (SIF) without enzyme pH 6.8, and phosphate buffer pH 7.4) on the optimized batch. Accurately weighed samples (n=3) equivalent to about 40 mg of papain were introduced to dissolution media and samples of 2 ml were collected at 0, 0.25, 0.50, 0.75, 1.0, 1.5, 2.0, 2.5, 3.0, 3.5, 4.0, 4.5, 5.0, 5.5 and 6.0 hr. Samples were filtered through whatman[®] filter paper #42 and assayed for enzyme content as before.

8.2.6.6. Fourier transform infra-red spectroscopy (FTIR)

IR transmission spectra were obtained using a FTIR spectrophotometer (FTIR-8300, Shimadzu, Japan). A total of 2% (w/w) of sample, with respect to the potassium bromide (KBr; S. D. Fine Chem Ltd., Mumbai, India) disc, was mixed with dry KBr. The mixture was ground into a fine powder using an agate mortar before compressing into KBr disc under a hydraulic press at 10,000 psi. Each KBr disc was scanned 16 times at 4 mm/s at a resolution of 2 cm^{-1} over a wavenumber region of $400\text{--}4000\text{ cm}^{-1}$ using Happ-Genzel apodization. The characteristic peaks were recorded.

8.2.6.7. Differential scanning calorimetry (DSC)

Differential scanning calorimetric analysis was used to characterize the thermal behavior of the isolated substances, empty and enzyme loaded beads. DSC thermograms were obtained using an automatic thermal analyzer system (DSC-60, Shimadzu, Japan). Temperature calibration was performed using indium as a standard. Samples were crimped in a standard aluminum pan and heated from $40\text{--}400\text{ }^{\circ}\text{C}$ at a heating rate of $10\text{ }^{\circ}\text{C}/\text{min}$ under constant purging of dry nitrogen at $30\text{ ml}/\text{min}$. An empty pan, sealed in the same way as the sample, was used as a reference.

8.2.6.8. Scanning electron microscopy (SEM)

The purpose of SEM study was to obtain a topographical characterization of the beads. The beads were mounted on brass stubs using carbon paste. SEM photographs were taken with scanning electron microscope (JSM-5610LV, Jeol Ltd., Tokyo, Japan) at the

required magnification at room temperature. The working distance of 39 mm was maintained and acceleration voltage used was 20 kV, with the secondary electron image (SEI) as a detector.

8.2.7. PREPARATION OF CAPSULE FORMULATION, PACKAGING, AND STABILITY STUDY

Accurately weighed chitosan-alginate beads equivalent to 40 mg of papain were filled into a hard gelatin capsule manually. The joint of the capsule body and cap was carefully sealed by pressing them to fit in the lock mechanism. The capsules were packed in high density polyethylene (HDPE) bottles with polypropylene (PP) caps (foamed polyethylene and pressure sensitive liner). The capsules were subjected to stability testing according to the International Conference on Harmonization guidelines for zone III and IV. The packed containers of prepared capsules along with marketed formulation and bulk papain were kept for accelerated ($40\pm 2^{\circ}\text{C}/75\pm 5\%$ relative humidity) and long term ($30\pm 2^{\circ}\text{C}/65\pm 5\%$ relative humidity) stability for up to 12 months. For accelerated and long term stability, desiccators containing saturated sodium chloride and potassium iodide solutions were kept into ovens at 40°C and 30°C to maintain a constant relative humidity of 74.68 ± 0.13 and 67.98 ± 0.23 , respectively. A visual inspection (for discoloration of capsule content), dissolution testing, and papain content estimation was carried out every 15 days for the entire period of stability study.

8.3. References

- AN, H., SEYMOUR, T. A., WU, J. W. and MORRISSEY, M. T., 1994. Assay systems and characterization of Pacific whiting (*Merluccius productus*) protease. *J. Food Sci.* 59, 277-281.
- BOX, G. E. P. and HUNTER, J. S., 1957. Multi-factorial designs for exploring response surfaces. *Ann. Math. Stat.* 28, 195-241.
- DERRINGER, G. and SUICH, R., 1980. Simultaneous optimization of several responses variables. *J Qual Technol* 2, 214-219.
- GIBALDI, M. and FELDMAN, S., 1967. Establishment of sink conditions in dissolution rate determinations - theoretical considerations and application to non-disintegrating dosage forms. *J. Pharm. Sci.* 56, 1238-1242.
- HIGUCHI, T., 1963. Mechanism of sustained-action medication. Theoretical analysis of rate of release of solid drugs dispersed in solid matrices. *J. Pharm. Sci.* 52, 1145-1149.
- HINTZE, J., NCSS and PASS ver. 2003, *Number Cruncher Statistical Systems*, Kaysville, Utah, www.ncss.com, 2003.
- HIXSON, A.W. and CROWELL, J.H., 1931. Dependence of reaction velocity upon surface and agitation. *Ind. Eng. Chem.* 23, 923-931.
- HSIU, JULIA, FISCHER, EDMOND H. and STEIN, ERIC A., 1964. Alpha-amylase as calcium-metalloenzymes. II. Calcium and the catalytic activity. *Biochemistry* 3, 61-66.
- KOPCHA, M., LORDI, N. and TOJO, K.J., 1991. Evaluation of release from selected thermosoftening vehicles. *J. Pharm. Pharmacol.* 43, 382-387.
- KORSMEYER, R.W., GURNY, R., DOELKER, E.M., BURI, P. and PEPPAS, N.A., 1983. Mechanism of solute release from porous hydrophilic polymers. *Int. J. Pharm.* 15, 25-35.

- PATHER, S. INDIRAN, RUSSELL, IRINA, SYCE, JAMES A. and NEAU, STEVEN H., 1998. Sustained release theophylline tablets by direct compression Part 1: formulation and in vitro testing. *Int. J. Pharm.* 164, 1-10.
- PEPPAS, N.A., 1985. Analysis of Fickian and non-Fickian drug release from polymers. *Pharm. Acta Helv.* 60, 110-111.
- PLACKETT, R. L. and BURMAN, J. P., 1946. The design of optimum multifactorial experiments. *Biometrika* 33, 305-325.
- RICE, EUGENE W., 1959. Improved spectrophotometric determination of amylase with a new stable starch substrate solution. *Clin. Chem.* 5, 592-596.
- RITGER, P. L. and PEPPAS, N. A., 1987. A simple equation for description of solute release II. Fickian and anomalous release from swellable devices. *J. Controlled Release* 5, 37-42.
- SHIGEO, O., TOSHIHIKO, K., YOUSUKE, M., HOROSHIMA, S., KOZO, T. and NAGAI, T., 1994. A new attempt to solve the scale up problem for granulation using response surface methodology. *J. Pharm. Sci.* 83, 439-443.
- SMITH, BENJAMIN W. and ROE, JOSEPH H., 1957. A micromodification of the Smith and Roe method for the determination of amylase in body fluids. *J. Biol. Chem.* 227, 357-362.
- TAYLOR, MICHAEL K., GINSBURG, JERI, HICKEY, ANTHONY J. and GHEYAS, FERDOUS, 2000. Composite method to quantify powder flow as a screening method in early tablet or capsule formulation development. *AAPS PharmSciTech* 1, article 18.
- TSUCHIDA, E., 1994. Formation of polyelectrolyte complexes and their structures. *J. Macromol. Sci. Pure Appl. Chem.* A31, 1-15.
- WAGNER, J. G., 1969. Interpretation of percent dissolved-time plots derived from In vitro testing of conventional tablets and capsules. *J. Pharm. Sci.* 58, 1253-1257.